Brain, Behavior, & Immunity - Health 30 (2023) 100638

Contents lists available at ScienceDirect

Brain, Behavior, & Immunity - Health

journal homepage: www.editorialmanager.com/bbih/default.aspx

# Ovariectomy in mice primes hippocampal microglia to exacerbate behavioral sickness responses☆

Kevin Sanchez, Sienna L. Wu, Reha Kakkar, Jeffrey S. Darling, Claire S. Harper, Laura K. Fonken *

*Division of Pharmacology & Toxicology, College of Pharmacy, The University of Texas at Austin, Austin, TX, 78712, USA*

ARTICLE INFO

*Keywords:*
Microglia
Estrogen
Ovariectomy
Lipopolysaccharide
Neuroinflammation
Sickness
Anxiety
Hippocampus

ABSTRACT

Estrogens are a group of steroid hormones that promote the development and maintenance of the female reproductive system and secondary sex characteristics. Estrogens also modulate immune responses; estrogen loss at menopause increases the risk of inflammatory disorders. Elevated inflammatory responses in the brain can lead to affective behavioral changes, which are characteristic of menopause. Thus, here we examined whether loss of estrogens sensitizes microglia, the primary innate immune cell of the brain, leading to changes in affective behaviors. To test this question, adult C57BL/6 mice underwent an ovariectomy to remove endogenous estrogens and then received estradiol hormone replacement or vehicle. After a one-month recovery, mice received an immune challenge with lipopolysaccharide (LPS) or vehicle control treatment and underwent behavioral testing. Ovariectomized, saline-treated mice exhibited reduced social investigation compared to sham-operated mice. Furthermore, ovariectomized mice that received LPS exhibited an exacerbated decrease in sucrose preference, which was ameliorated by estradiol replacement. These results indicate that ovariectomy modulates affective behaviors at baseline and in response to an inflammatory challenge. Ovariectomy-related behavioral changes were associated with downregulation of *Cx3cr1*, a microglial receptor that limits activation, suggesting that estrogen loss can disinhibit microglia to immune stimuli. Indeed, estradiol treatment reduced ovariectomy-induced increases in *Il1b* and *Il6* expression after an immune challenge. Changes in microglial reactivity following ovariectomy are likely subtle, as overt changes in microglial morphology (e.g., soma size and branching) were limited. Collectively, these results suggest that a lack of estrogens may allow microglia to confer exaggerated neuroimmune responses, thereby raising vulnerability to adverse affective- and sickness-related behavioral changes.

## 1. Introduction

The immune system functions in a sexually dimorphic manner — females tend to have more robust inflammatory responses than males (Klein and Flanagan, 2016; Yang and Kozloski, 2011). Furthermore, immune responses change over the lifetime in females. Menopause increases the risk for inflammatory disorders, likely due to loss of estrogens. Estrogen signaling regulates the development, differentiation, and function of various immune cells (Villa et al., 2016). In addition to regulating peripheral inflammatory responses, estrogens can modulate changes in the neuroimmune environment and have classically been considered neuroprotective against injury or damage to the central nervous system. The mechanisms by which estrogens modulate the neuroimmune environment to protect against inflammatory diseases are not fully understood but likely involve changes in microglia, the predominant brain-resident immunocompetent cell. Microglia express estrogen receptors (e.g., ERα, ERβ, and G protein-coupled estrogen receptor; Acosta-Martinez, 2020), and estrogens can suppress microglial inflammatory responses (Ghisletti et al., 2005; Kopitar-Jerala, 2015; Murphy et al., 2010; Vegeto et al., 2003).

Microglial activation, and the subsequent release of pro-inflammatory cytokines, can drive a suite of physiological and behavioral alterations, termed the sickness response. Behavioral characteristics of this response include reduced food intake, social withdrawal, anhedonia, and cognitive impairments (Hennessy et al., 2014; Henry et al., 2008; Szentirmai and Krueger, 2014; Zhao et al., 2019). While

☆ Present address: 107 W Dean Keeton St 3.510C, Austin, TX 78712.
* Corresponding author.
*E-mail address:* laura.fonken@austin.utexas.edu (L.K. Fonken).

https://doi.org/10.1016/j.bbih.2023.100638
Received 5 December 2022; Received in revised form 14 April 2023; Accepted 7 May 2023
Available online 18 May 2023

these sickness behaviors function as short-term adaptations by putatively helping an organism recover from infection or injury (Hart, 1988), the chronic neuroinflammation associated with the long-term expression of these behaviors is maladaptive (Dantzer et al., 2008). Indeed, long-term neuroinflammation increases vulnerability to affective and cognitive disorders (Colpo et al., 2018; Gabbita et al., 2012; Kim et al., 2016; Kokiko-Cochran and Godbout, 2018; Rhie et al., 2020). For example, traumatic brain injury can modulate the neuroimmune system and cause marked behavioral changes reminiscent of the aforementioned sickness behaviors (Muccigrosso et al., 2016; Niraula et al., 2017; Tapp et al., 2019). A second challenge is often required to expose these neuroimmune alterations, frequently leading to the exacerbated microglial release of pro-inflammatory molecules that may contribute to affective disorders and cognitive decline. This concept of neuroimmune "priming," or sensitizing, occurs in several contexts, such as stress, aging, sleep deprivation (Bellesi et al., 2017; Espinosa-Garcia et al., 2017; Niraula et al., 2017), yet it is unclear if estrogen loss can prime the neuroimmune system to an immune stimulus. Specifically, there is limited work assessing whether estrogen loss can induce features of microglial reactivity (e.g., morphological and gene expression changes) at baseline and after an immune challenge. For example, it remains unknown whether estrogen loss can reduce expression of receptors known to suppress microglial reactivity (e.g., the fractalkine receptor, CX3CR1). Blunted expression of these receptors can disinhibit microglia to a subsequent immune stimulus, exacerbating neuroinflammation and behavioral deficits.

Importantly, women are twice as likely to be diagnosed with depression than men (Kessler, 2003; Rubinow and Schmidt, 2019), and this risk is amplified following estrogen loss (Sagsoz et al., 2001). This increased susceptibility may occur due to diminished interactions between estrogens and neuroimmune cells such as microglia (Hara et al., 2015; Schwarz and Bilbo, 2012; Villa et al., 2016). After pathological insult (e.g., exposure to a pathogen, traumatic brain injury), estrogens promote neuronal survival, inhibit neuroinflammation, and facilitate repair of damaged neural tissue (Hara et al., 2015; Villa et al., 2016).

Here, we hypothesized that estrogen loss could prime the neuroimmune system, exacerbating the release of pro-inflammatory mediators that may worsen behavioral deficits. Our results demonstrate that ovariectomy (OVX) in mice leads to social withdrawal and exacerbated sickness behaviors. These behavioral deficits were accompanied by changes in gene expression indicative of disinhibition of microglia and amplified neuroinflammation in the hippocampus. Our results suggest that estrogen loss in mice may increase neuroinflammatory priming and sickness behaviors, which could have implications for women following menopause.

## 2. Materials and methods

### 2.1. Animals

Four-month-old female C57BL/6 mice were ordered from The Jackson Laboratories. Mice were housed in standard polycarbonate cages on Sani-Chips bedding (i.e., hardwood shavings) and reverse osmosis filtered water and food (Prolab RMH, 1800; LabDiet) were provided *ad libitum*. All mice were group housed prior to surgery and post-surgery mice were either individually housed (for behavioral testing) or pair-housed (for gene expression). Throughout the study, mice were housed in a temperature-controlled (20 ± 2 °C) room with a 12 h light/dark cycle (lights on at 0300 h). Mice were acclimated to the facility for one week prior to experimental manipulations. All experiments were conducted following NIH guidelines, approved by The University of Texas Institutional Animal Care and Use Committee, and performed in accordance with ARRIVE guidelines.

### 2.2. Ovariectomy

Four-month-old mice received an OVX or sham operation. Mice were anesthetized with 5% isoflurane (Patterson Veterinary) in oxygen and then maintained on 1.5–2% isoflurane during the procedure. All mice received a 100 μg/kg subcutaneous injection of buprenorphine (Par Pharmaceutical) before the operation. The surgical site was shaved and then cleaned by applying 70% ethanol and betadine. A single incision down the posterior midline was made, and two internal muscle wall incisions were made directly over the ovaries to extract them. The same incisions occurred in mice receiving the sham operation, but the ovaries were left intact. Absorbable sutures (6-0, AD Surgical) were then used to close the superficial fascia. Nylon sutures (6-0, AD Surgical) were utilized to close the external incision. As confirmation of successful OVX, the absence of ovaries was noted during euthanasia for all cohorts. Additionally, uterine horn mass was taken from all mice by cutting through the oviduct-uterine horn junction, through the uterine fundus, and towards the contralateral oviduct-uterine horn junction.

### 2.3. Hormone replacement

Following a one-week recovery from the surgery, mice received 50 μL subcutaneous injections of either sesame oil (vehicle [V]; Sigma) or 1 μg estradiol ($E_2$; Sigma). Injections were provided every four days to mimic their endogenous estrous cycle for 40 days (Gresack and Frick, 2006). Moreover, these injections were always provided between 1400 h and 1500 h (i.e., 1 h before lights off) since $E_2$ exhibits a circadian rhythm with a peak at the onset of the active phase (Butler, 2018). Mice were weighed during each hormone injection.

### 2.4. Behavioral assessment

A subset of mice completed a series of behavioral tests following the 40 days of hormone replacement at 5.5 months old. These tests were conducted after an inflammatory response was induced by an intraperitoneal injection of lipopolysaccharide (LPS; 500 μg/kg; Sigma, *E. coli* serotype 0111:B4) or 0.9% saline. This LPS dose is commonly used to investigate the mechanisms underlying affective disorders, since LPS-elicited inflammation can amplify or expose behavioral alterations (Dang et al., 2019; Tarr et al., 2012; Zhao et al., 2019). Behavioral analyses in an open field and juvenile social exploration test occurred 6 h following LPS injection. In addition, sucrose preference was measured from 8 to 14 h post-LPS or saline injection. These behavior tests were all performed in the dark phase, commencing at 1800 h.

#### 2.4.1. Open field test

Mice were placed into an unfamiliar, inescapable square arena (50 $cm^3$) for 5 min. The central area is considered more anxiogenic relative to the edges (Seibenhener and Wooten, 2015). Anxiety-like behavior was measured as the time spent in the center of the open field. The arena was wiped down with 70% ethanol and allowed to air dry between mice. Exploratory behavior was scored using automated tracking with EthoVision software.

#### 2.4.2. Juvenile social exploration

Directly following the open field test, a juvenile mouse (sex-matched and 28 ± 3 days old) was added to the open field arena for 5 min to observe social behavior. Behavior was recorded using EthoVision software and a condition-blinded experimenter manually scored time spent investigating the juvenile (e.g., sniffing, pinning, allogrooming, chasing). Decreased interaction time initiated by the test mouse is indicative of increased anxiety-like behavior (Bailey and Crawley, 2009).

#### 2.4.3. Sucrose preference test

Each mouse received two bottles, one containing water and the other

a 2% sucrose (Sigma) solution. Mice were acclimated to the two-choice test for 6 h during the dark phase for two nights before the LPS or saline injection. Sucrose intake was measured to determine the percentage of preference for sucrose water over regular water. Eight hours after the LPS or saline injection, sucrose preference was observed to reveal if the LPS inflammatory response impacted anhedonia (Scheggi et al., 2018).

### 2.5. Immunohistochemistry

Twenty-four hours following the LPS or saline injection, mice were euthanized with a lethal injection of a sodium pentobarbital-containing solution (Euthasol, Med-Pharmex). Once the mice were unresponsive, they were perfused transcardially with phosphate-buffered saline (PBS) followed by 4% paraformaldehyde (Sigma). Brains were removed and post-fixed overnight with 4% paraformaldehyde, cryoprotected in 30% sucrose, frozen with isopentane (Acros Organics) on dry ice at −55 °C, and stored at −80 °C. Brains were subsequently sectioned onto Fisher Superfrost Plus slides at 20 μm using a cryostat at −23 °C and stored in a −20 °C freezer.

For immunohistochemistry, slides were blocked with 10% normal goat serum in 1x PBS +0.2% Triton X-100 for 1 h at room temperature. Slides were incubated overnight with rabbit anti-Iba1 antibody (1:1000; Wako; RRID: AB_839504) in blocking buffer at 4 °C. Slides were washed and then incubated in biotinylated secondary antibody (1:1000; Vector Laboratories; Catalog Number: BA-1000-1.5) for 1 h followed by an avidin-biotin horseradish peroxidase complex (Vector Laboratories; Catalog Number: PK-6100) for another hour. The sections were then incubated in diaminobenzidine (DAB; Vector Laboratories; Catalog Number: SK-4100) to visualize the horseradish peroxidase activity. This reaction was terminated when the contrast between the microglia and nonspecific background labeling was optimal (at 3 min). The sections were then dehydrated in a series of alcohols, cleared in xylene, and coverslipped with Permount.

### 2.6. Microglial morphological analyses

Morphological analyses of microglia were performed by a condition-blind observer using FIJI. The cornu ammonis 1 (CA1), CA3, and dentate gyrus (DG) subfields from the hippocampus were analyzed between Bregma −2.2 and −2.6 mm 20 μm-thick Z-stacked photomicrographs were acquired from an Olympus BX61 bright-field microscope at 1 μm intervals (20 images). This depth allows for complete reconstruction of the microglial soma and processes while avoiding overlap of microglia that would confound our analyses (Fernandez-Arjona et al., 2017). All analyses had four to seven mice per experimental group.

#### 2.6.1. Microglial density

Simple morphometric cell counting was performed using the "Cell Counter" plug-in on FIJI. Microglial counts were obtained by determining the number of cells and staining area from 10x DAB-stained images. Absolute cell count was then divided by the area analyzed (475,000 pixels$^2$ for the CA1 and CA3; 400,000 pixels$^2$ for the DG) to calculate the microglial density. All morphometric analyses were conducted by one trained experimenter blinded to experimental groups.

#### 2.6.2. Area fraction analysis

40x DAB-stained images were batch processed with a macro on FIJI (Young and Morrison, 2018). An "FFT Bandpass Filter" was first applied to remove background noise less than three pixels while preserving the larger qualities of the image. This was then converted into an 8-bit grayscale image before applying an "Unsharp Mask" filter that sharpens the image's features. A "Despeckle" step was then conducted to remove salt-and-pepper noise. The image was then auto-thresholded, converting it to a black and white image. A binary "Close" function that connects dark pixels if separated by up to two pixels was then applied. Finally, the "Remove Outliers" plug-in was used to eliminate background noise up to two pixels in size. The area fraction was then calculated. Every thresholded image was visually inspected to guarantee that an accurate area fraction was attained. If the automatic thresholding unsuccessfully removed the background noise, then the thresholding step was manually executed.

#### 2.6.3. Microglial soma characteristics

Microglial somas were traced on FIJI using the "Freehand Selections" tool utilizing a Huion Inspiroy H950P Graphics Drawing Tablet. 40x DAB-stained images were used, and 12 microglia were processed for each brain region. Soma perimeter was then calculated using FIJI by a condition-blind experimenter.

#### 2.6.4. Sholl and skeletonization analyses

40x DAB-stained images from the CA1 hippocampal subfield were processed by the same macro used for the area fraction analysis. Microglia were isolated, and background noise was eliminated. The "Paintbrush" tool was then used to fill in gaps between the microglial processes. The Sholl analysis was conducted using the "Sholl Analysis" plug-in on FIJI. The start radius was set at five pixels from the soma center, and the step size was defined as seven pixels. Microglial characteristics were assessed in five cells per animal across two to three sections and averaged to generate one value per animal for statistical analyses. Images were acquired on sections from either opposing hemispheres or adjacent brain slices. Only representative microglia that had well-defined somas and processes were chosen and processed.

### 2.7. Gene expression

After the 40 days of hormone replacement, a second subset of mice received an intraperitoneal LPS (500 μg/kg) or saline (control) injection. Six hours following the LPS or saline injection, mice were anesthetized with 5% isoflurane followed by decapitation. Using a cryostat at −18 °C, five 100 μm thick sections between Bregma −2.2 and −2.6 mm were sliced and mounted on a microscope slide. A 0.50 mm tissue micropunch (Stoelting) was subsequently used to obtain tissue from the CA1 hippocampal subfield. This brain region was selected as the hippocampus contains a high density of microglia and is implicated in regulating the affective and sickness behaviors evaluated in this study (Ivy et al., 2010; Price and Drevets, 2010). Additionally, our immunohistochemical analyses indicated morphological features were more consistently influenced by LPS and OVX in the CA1 relative to the other subfields.

CA1 hippocampal tissue was homogenized in TRIzol (Ambion), and RNA was isolated by performing a TRIzol-chloroform (Fisher) extraction (as described in Fonken et al., 2016). RNA was then reverse transcribed to cDNA using Superscript IV (Life Technologies) according to the manufacturer's instructions. PCR amplification of cDNA was performed using TaqMan reagents with a QuantStudio 3 detection system. Gene expression was determined in duplicate and expressed relative to *GAPDH*. There were no group differences in the housekeeping gene. All qRT-PCR results were analyzed using the $2^{-\Delta\Delta Ct}$ method and were normalized such that the control group was set to a value of 1. Gene expression of *Cx3cr1*, *Il1b*, *Il6*, *Stat3*, *Tnf*, and *Trem2* was determined through this method using inventoried TaqMan primers.

### 2.8. Statistical analyses

All data presented in the figures are expressed as mean ± standard error of the mean (SEM). Statistical analyses consisted of one-way (surgery) and two-way ANOVAs (surgery x sickness) between experimental groups. If there was a main effect of surgery or an interaction effect between surgery and sickness, Tukey's post hoc test was performed to correct for multiple comparisons. The analyses and generation of figures were performed using GraphPad Prism 9 and R.

## 3. Results

### 3.1. Ovariectomy is associated with increased body mass, uterine horn atrophy, and splenomegaly at baseline and after an immune challenge

Young adult female C57BL/6 mice underwent either a bilateral ovariectomy or sham operation and received $E_2$ replacement or vehicle of sesame oil every four days to mimic their estrous cycle (Fig. 1a). Consistent with prior findings, OVX mice gained more mass than the sham mice, starting at 11 days post-surgery (Kurachi et al., 1993; Rogers et al., 2009; Santollo et al., 2011; Vieira Potter et al., 2012). Administration of $E_2$ in OVX mice reduced the rate of body mass gain relative to OVX mice and, therefore, resulted in an intermediary body mass at the time of euthanasia ($F_{(2,118)} = 23.2$, $p < 0.05$; post hoc, $p < 0.05$; Fig. 1b). The increased body mass associated with OVX was paralleled by an elevation in ovarian white adipose tissue mass, which was 252% greater in OVX mice relative to sham mice ($F_{(2,45)} = 10.3$, $p < 0.05$; post hoc, $p < 0.05$). Moreover, there was significant atrophy of the uterine horn in the OVX mice that was not apparent in sham mice or OVX mice that received $E_2$ ($F_{(2,111)} = 142$, $p < 0.05$; post hoc, $p < 0.05$; Fig. 1c).

Forty days post-$E_2$ replacement or vehicle, mice were injected with LPS to induce an inflammatory response (Fig. 1a). As expected, there was a stark decrease in body mass 24 h after LPS administration, with these mice losing 10.8% of their body mass after 24 h (LPS, $F_{(1,46)} = 386$, $p < 0.05$; Fig. 1d). The masses of immune responsive organs, such as the adrenal glands and spleen, were also taken to further validate successful injection of LPS. Indeed, splenomegaly (LPS, $F_{(1,43)} = 83.1$, $p < 0.05$) and adrenal swelling (LPS, $F_{(1,43)} = 7.85$, $p < 0.05$) were observed in response to the immune challenge.

### 3.2. Ovariectomy impairs sociability and amplifies sickness behaviors

In the 24 h following the LPS injection, mice underwent a battery of behavioral tasks assessing sickness behaviors. Mice that received LPS exhibited reduced locomotor activity (LPS, $F_{(1,49)} = 218$, $p < 0.05$) and time spent in the center zone of the open field (LPS, $F_{(1,48)} = 69.9$, $p < 0.05$; Fig. 2a), consistent with a sickness response. Moreover, OVX vehicle-treated mice had a trend towards decreased central tendency compared to OVX mice that were administered $E_2$ (OVX, $F_{(2,48)} = 2.87$, $p = 0.066$; post hoc OVX + V vs. OVX + $E_2$, $p = 0.053$; Fig. 2a), suggesting that loss of estrogen may promote anxiety-like behaviors.

In the juvenile social exploration test, OVX mice had diminished social behaviors in the absence of an immune challenge, regardless of $E_2$ replacement status (LPS x OVX, $F_{(2,46)} = 6.27$, $p < 0.05$; post hoc, $p < 0.05$; Fig. 2b). Consistent with a sickness response, LPS-injected mice spent virtually no time investigating a juvenile mouse. In a sucrose preference task at baseline, all mice had a robust preference for the sucrose solution. Post-LPS, OVX mice consumed less of the sucrose solution compared to their sham and $E_2$ replacement counterparts, suggesting an exacerbated sickness response (LPS x OVX, $F_{(2,50)} = 3.94$, $p < 0.05$; post hoc, $p < 0.05$; Fig. 2c). These results indicate that although estrogens may not mediate the social impairments observed following OVX, estrogen loss appears to play a role in aggravating the sickness response.

### 3.3. Ovariectomy primes microglia in the CA1 hippocampal subfield

We next assessed whether there were alterations in the expression of genes from the CA1 hippocampal subfield since this brain region is associated with the behavioral sickness response and has a high density of microglia (Askew et al., 2017; Lawson et al., 1990; Liu et al., 2018; Savage et al., 2019). To better characterize whether estrogen loss can influence microglial dynamics and crosstalk with neurons, the expression of the fractalkine receptor, *Cx3cr1*, and triggering receptor expressed on myeloid cells 2 (*Trem2*) were assessed. OVX mice had downregulated expression of *Cx3cr1* at baseline that was rescued by $E_2$ replacement (LPS x OVX, $F_{(2,26)} = 4.89$, $p < 0.05$; post hoc, $p < 0.05$). Similarly, there was decreased expression of *Trem2* in OVX mice that was restored by administration of $E_2$ in the absence of an immune stimulus (LPS x OVX, $F_{(2,31)} = 7.05$, $p < 0.05$; post hoc, $p < 0.05$).

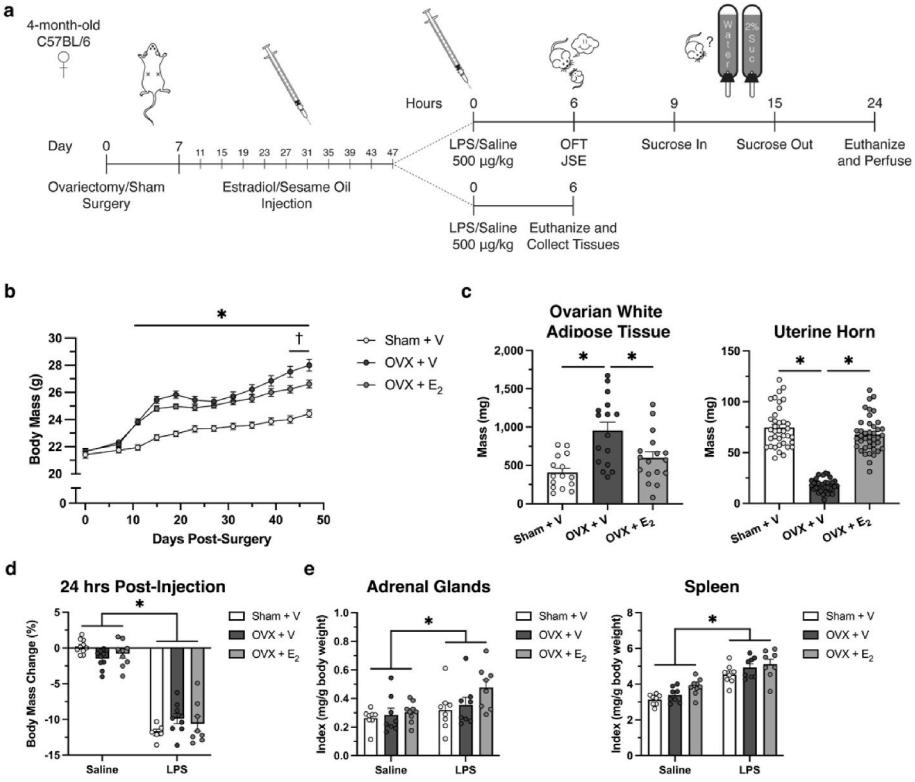


**Fig. 1. Ovariectomized mice have elevated body mass, uterine horn atrophy, and splenomegaly. a,** Experimental timeline illustrating the timing of surgery, estradiol replacement, and behavior testing paradigm. **b,** Ovariectomized mice gained more body mass throughout the experiment (n = 39–42/group). **c,** Ovariectomy results in elevated deposits of white adipose tissue around the ovaries (n = 15–17/group) and uterine horn atrophy (n = 36–41/group). **d,** After a lipopolysaccharide (LPS) injection, there is a substantial decrease in body mass 24 h (n = 6–10/group) after injection. **e,** Enlargement of the adrenal gland and spleen relative to body mass is observed in response to LPS (n = 8–9/group). The data are graphed as mean ± SEM; * — $p < 0.05$ (main effect of sickness), $p < 0.05$ (Tukey's post hoc test), or $p < 0.05$ Sham + V vs. OVX + V; † — $p < 0.05$ OVX + V vs. OVX + $E_2$.

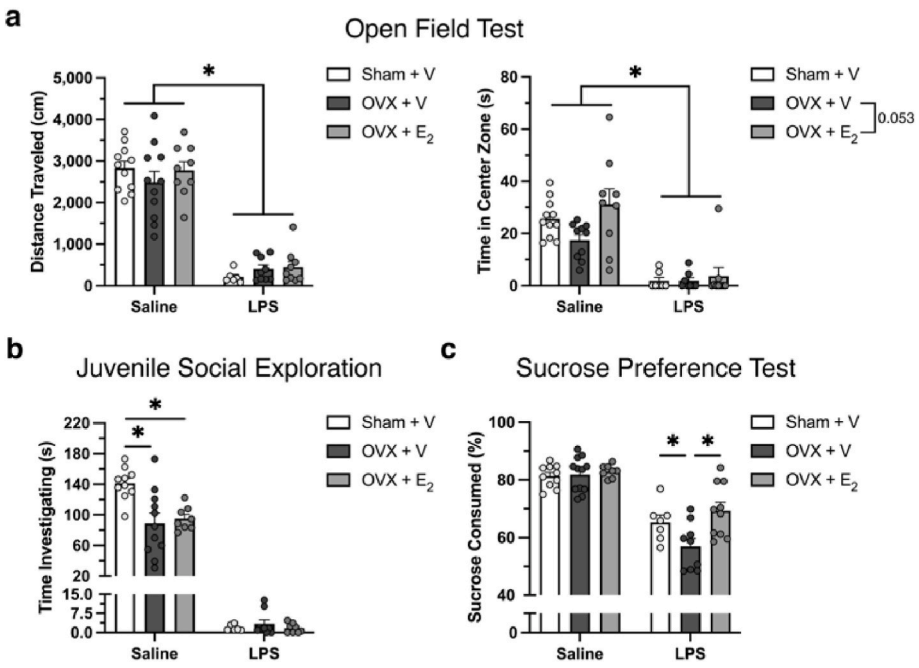


**Fig. 2. Affective behavioral deficits are present in ovariectomized mice at baseline and after an immune challenge. a,** Locomotor activity during the 5-min open field test was substantially decreased after a lipopolysaccharide (LPS) injection. Ovariectomized mice tended to spend less time in the anxiogenic center zone of the open field compared to those that received estradiol replacement. Minimal time was spent in the center zone across all groups after an immune challenge. **b,** Ovariectomy, independent of estradiol replacement, leads to impaired sociability in the juvenile social exploration test. An infinitesimal amount of sociability was recorded after an LPS injection. **c,** Ovariectomized mice consumed less sucrose after an immune challenge than sham mice and those with estradiol replacement, suggestive of exacerbated sickness behaviors. The data are graphed as mean ± SEM; n = 6–12/group; * — $p < 0.05$ (main effect of sickness), $p < 0.05$ (Tukey's post hoc test).

Interestingly, OVX mice had elevated *Trem2* expression after an LPS challenge relative to mice given $E_2$ (post hoc, $p < 0.05$; Fig. 3a). These data suggest that loss of estrogen may disinhibit microglia and facilitate exacerbated neuroinflammation following an immune response.

Next, the expression of pro-inflammatory-related mRNAs was assessed to determine whether OVX mice had amplified inflammation due to a primed neuroimmune system. LPS upregulated expression of *Il1b* and *Tnf* in the CA1 subfield across all experimental groups (LPS,

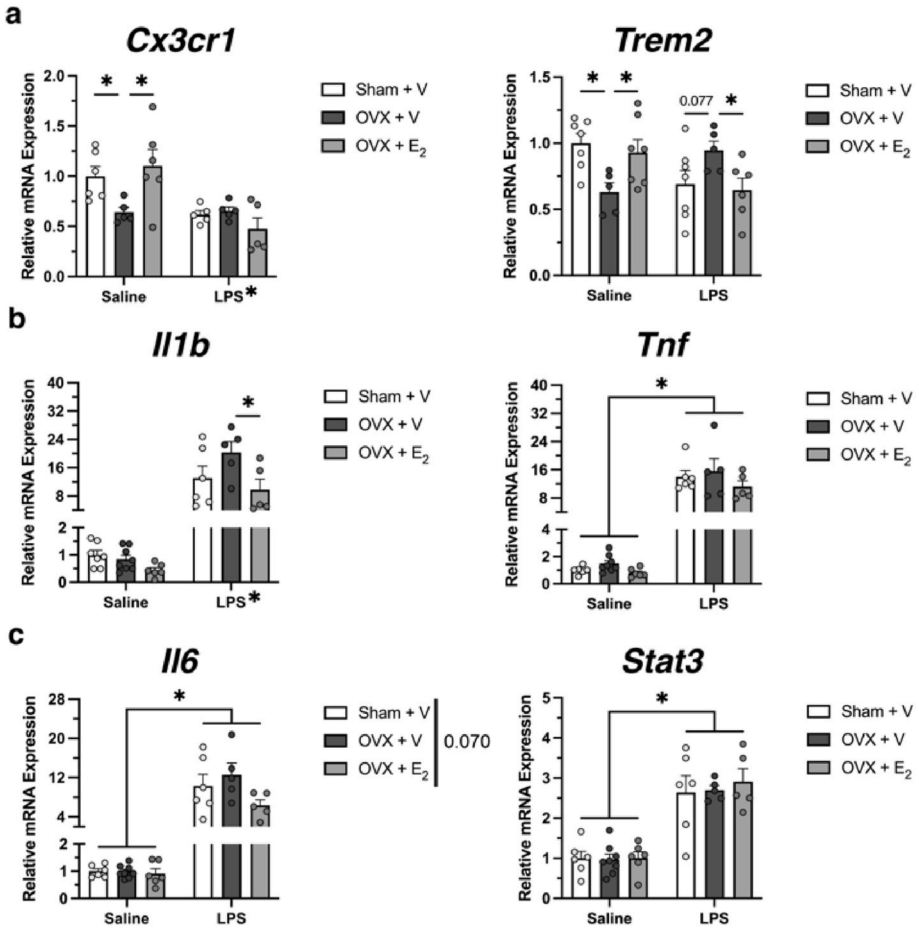


**Fig. 3. Ovariectomized mice display priming of microglia and exacerbated hippocampal expression of Il6. a,** Expression of microglial anti-inflammatory markers Cx3cr1 and Trem2 were diminished at baseline in ovariectomized mice, suggestive of microglial priming, and ameliorated with estradiol. **b,** Estradiol administration prevented ovariectomy-induced increases in Il1b expression after an immune challenge with lipopolysaccharide (LPS). Tnf expression was upregulated with LPS. **c,** Il6 and Stat3 expression are amplified after an LPS injection. The data are graphed as mean ± SEM; n = 5–8/group; * — $p < 0.05$ (main effect of sickness), $p < 0.05$ (Tukey's post hoc test).

[*Il1b*] $F_{(1,31)} = 73.2$, [*Tnf*] $F_{(1,30)} = 99.9$, $p < 0.05$). $E_2$ administration significantly reduced OVX-associated increases in *Il1b* expression after an immune challenge (LPS x OVX, $F_{(2,31)} = 3.53$, $p < 0.05$; post hoc, $p < 0.05$; Fig. 3b). Similar to *Il1b* and *Tnf*, expression of *Il6* was elevated following an immune challenge (LPS, $F_{(1,30)} = 67.5$, $p < 0.05$). Moreover, mice receiving $E_2$ replacement tended to have diminished *Il6* expression compared to OVX mice receiving vehicle (OVX, $F_{(2,30)} = 2.90$, $p = 0.070$; post hoc, $p = 0.059$). The expression of *Stat3*, a transcription factor downstream of IL6, was also elevated with LPS (LPS, $F_{(1,30)} = 79.9$, $p < 0.05$) but was not affected by OVX ($p > 0.05$; Fig. 3c). Altogether, these results suggest that estrogens may aid in quenching the release of pro-inflammatory IL-1β and IL6 in response to an immune stimulus.

### 3.4. Ovariectomy produces limited changes in microglia density and morphology in the hippocampus

Given that OVX mice showed signs of microglial priming in the hippocampus, we next sought to determine whether OVX altered microglial morphology. Twenty-four hours following the LPS or saline injection, brains were collected, sliced, and stained with DAB against Iba1 to visualize microglia in CA1, CA3, and DG hippocampal subfields (Fig. 4a). We first assessed whether differences in microglial density were apparent between our groups. In the CA1, OVX mice had more microglia than OVX mice which received $E_2$ replacement (OVX, $F_{(2,26)} = 5.35$, $p < 0.05$; post hoc, $p < 0.05$). Administration of LPS increased microglial density in the DG (LPS, $F_{(1,26)} = 5.07$, $p < 0.05$). Moreover, DG microglial density was elevated in OVX mice relative to sham mice (OVX, $F_{(2,26)} = 5.48$, $p < 0.05$; post hoc sham + V vs. OVX + V, $p < 0.05$; Fig. 4b).

Next, area fraction analysis was conducted to determine whether OVX or LPS administration altered density of Iba1 immunoreactivity (Yew et al., 2019). Microscopy images were first pre-processed to remove background noise before being thresholded for calculating the area fraction (Fig. 4a). Similar to our microglial density results, OVX mice had elevated Iba1 immunoreactivity compared to OVX mice that received $E_2$ in the CA1 subfield (OVX, $F_{(2,28)} = 3.54$, $p < 0.05$). Additionally, LPS-injected mice had an overall increase in $Iba1^+$ staining in both the CA1 and DG subfields (LPS, [CA1] $F_{(1,28)} = 5.68$, [DG] $F_{(1,28)} = 8.64$, $p < 0.05$; Fig. 4c). Importantly, microglial density and Iba1

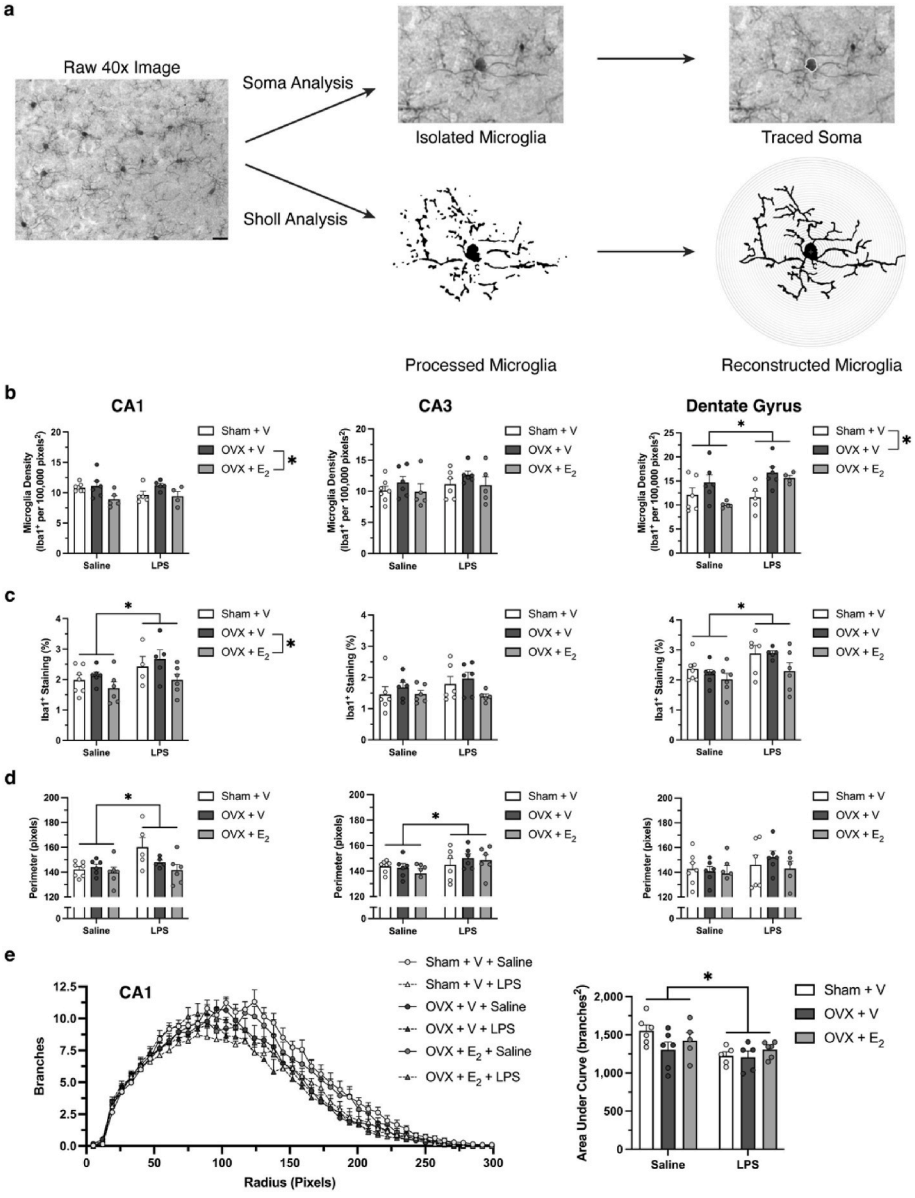


**Fig. 4. Ovariectomy increases the density of microglia in the hippocampus but doesn't affect morphology. a,** Methodology for assessing microglial soma morphological features (top) and microglial branching complexity (bottom). **b,** Microglial density analysis indicates that ovariectomized mice have greater recruitment of microglia in the CA1 and dentate gyrus than mice that received estradiol replacement and sham operations, respectively. **c,** Iba1 immunoreactivity is elevated in the CA1 and dentate gyrus following an immune challenge. **d,** The perimeter of outlined microglial somas in the CA1 and CA3 subfields were enlarged in response to lipopolysaccharide (LPS) treatment (12 microglia/mouse). **e,** Plotting branches vs. radius from soma reveals differential changes in microglial branching due to lipopolysaccharide administration. Global differences in microglial complexity were assessed with an area under the curve analysis that indicated deramification of processes after a LPS injection (5 microglia/mouse). The data are graphed as mean ± SEM; n = 4–7/group; scale bar = 20 μm; * — $p < 0.05$ (main effect of sickness), $p < 0.05$ (Tukey's post hoc test).

immunoreactivity are often used as a first pass to assess gross changes in microglial morphology; however, these parameters do not detect subtle changes nor the subcellular localization of these alterations (e.g., soma or processes). Thus, we next performed microglial morphological analyses for soma characteristics and branching complexity.

In response to an immune stimulus, microglial somas swell and become more jagged, leading to an increase in soma perimeter (Davis et al., 2017). As expected, LPS elicited soma swelling the CA1 and CA3 subfields (LPS, [CA1] $F_{(1,29)} = 3.56$, [CA3] $F_{(1,31)} = 4.31$, [CA1] $p = 0.069$, [CA3] $p < 0.05$; Fig. 4d). No difference in soma perimeter was noted in the DG ($p > 0.05$).

We next assessed the effects of LPS and OVX on microglial branching and complexity in the CA1 subfield. This region was selected as morphological features were more consistently influenced by LPS and OVX relative to the CA3 and DG (Fig. 4b–d). Microscopy images were first processed with a FIJI macro to binarize the image and isolate microglia. Processes were then manually drawn while referencing the raw image for subsequent Sholl and skeletonization analyses (Fig. 4a). LPS administration led to reduced branching across all distances from the soma in an area under curve analysis (LPS, $F_{(1,29)} = 7.64$, $p < 0.05$; Fig. 4e). OVX had no significant effect on these morphologic indicators of microglial reactivity ($p > 0.05$). Collectively, these microglial morphological results indicate that OVX increases microglial density in the hippocampus, and that estrogens do not significantly regulate reactivity-related characteristics of the microglial soma and processes.

## 4. Discussion

Estrogen loss increases the risk for chronic inflammatory diseases as well as mood disorders (Au et al., 2016; Vegeto et al., 2008; Villa et al., 2016). Increases in inflammatory responses in the brain (i.e., neuroinflammation) can shift mood-related behaviors. Thus, here we investigated whether estrogen loss can regulate behavior through sensitizing microglia. OVX mice had elevated anxiety-like behaviors and amplified sickness responses that were partly abrogated by $E_2$ administration. Gene expression analyses suggest that OVX may lead to the disinhibition of microglia (e.g., reduced *Cx3cr1)*. Despite this, OVX did not impact microglial soma morphology or microglial branching complexity. Upon an immune challenge with LPS, OVX mice had a greater neuroimmune response in the hippocampus that likely contributes to the observed sickness behaviors in OVX rodents. Altogether, these data suggest that estrogen loss following OVX may prime hippocampal microglia to a subsequent immune challenge and that $E_2$ replacement can ameliorate this exacerbated neuroinflammation and related behavioral impairments.

Consistent with prior studies, systemic LPS injection led to a robust sickness response characterized by body mass loss, sickness behaviors, and neuroinflammation (Henry et al., 2008; Yeh et al., 2018). Microglia primarily mediate this sickness response by inducing the release of pro-inflammatory cytokines, including IL-1β, IL-6, and TNF-α (Dantzer et al., 2008; Lenz and McCarthy, 2015). Indeed, we observed an LPS-induced increase in the mRNA expression of these cytokines in mouse hippocampus.

The heightened hippocampal neuroinflammatory response following the LPS injection was accompanied by behavioral changes. LPS-injected mice had decreased exploration of an open field, minimal time investigating a juvenile mouse, and a reduction in sucrose preference. OVX increased sickness behaviors following an LPS challenge, specifically in a sucrose preference test. Furthermore, decreases in sucrose preference among OVX mice were rescued by replacement with $E_2$. The enhanced sickness response in OVX mice may result from a disinhibited neuroimmune system. mRNA expression of the fractalkine receptor, *Cx3cr1*, was reduced in OVX mice. CX3CR1 is a microglial receptor bound by the neuronal fractalkine ligand (i.e., CX3CL1); this receptor:ligand interaction maintains microglia in a homeostatic surveillant state (Pawelec et al., 2020). Disrupted signaling of the CX3CL1:CX3CR1 axis can lead to disinhibition of microglia leading to hyperactivation in response to an immune stimulus (Niraula et al., 2017; Wolf et al., 2013). Indeed, LPS-injected OVX mice had increased *Il1b* gene induction. Importantly, mRNA expression does not necessarily correlate with functional protein expression. Therefore, future studies examining how estrogens impact protein levels of inflammatory cytokines should perform pertinent protein expression assays (e.g., multiplex assays, ELISAs, Western blots) (Posillico et al., 2021). Of note, the behavioral response to LPS was robust, which likely produced a near-maximal effect where it was not possible to detect any modulation of the sickness response by OVX. For example, mice administered LPS had minimal locomotor activity in the open field test that led to almost no time exploring the center zone of the arena or another juvenile mouse. Prior work focusing on neuroinflammatory priming in contexts such as stress used a lower LPS dose (e.g., 100–330 μg/kg) to detect an amplified sickness response (Henry et al., 2009; Mizobuchi and Soma, 2021; O'Neil et al., 2018). Usage of this dose can unmask behavioral deficits, such as decreased social exploration (O'Neil et al., 2018).

In addition to the production of estrogens, the ovaries are involved in the synthesis and release of progesterone ($P_4$) and androgens (McNatty et al., 1979). Consequently, OVX also blunts these sex hormone concentrations, and some of the investigated behaviors may be additionally regulated by these other hormones. Indeed, although $E_2$ replacement reverted many of the physiological, behavioral, and neuroimmune impairments induced by OVX, this was not the case for all investigated parameters. In the juvenile social exploration test, saline-treated OVX mice exhibited reduced social exploration that $E_2$ could not restore, suggesting that other hormones may be at play in regulating social behaviors. For example, in both female humans and rodents, elevated levels of $P_4$ are associated with increased social behaviors (e.g., social closeness, social monitoring, social play) (Brown et al., 2009; Forbes-Lorman, 2021; Frye et al., 2009; Maner and Miller, 2014).

Microglial morphology is highly dynamic, with subtle changes in microenvironment leading to shifts in morphology. For example, prior work indicates that "priming" (e.g., due to aging) or "activation" (e.g., infection, injury) of microglia can induce morphological changes, such as soma swelling and reduced branching complexity (Campagno et al., 2021; Davis et al., 2017; Sanchez et al., 2022). Here we show that somas from hippocampal microglia had increased perimeter post-LPS; however, this effect was only noted in the CA subfields and not in the DG. Immune challenges also cause acute increases in microglial density (Benusa et al., 2020; Velez-Perez et al., 2020). In agreement with prior work, LPS treatment elevated microglial density, specifically in the DG. Furthermore, OVX was associated with greater accumulation of microglia in the CA1 and DG. This higher density of microglia could have contributed to the exacerbated LPS-elicited hippocampal neuroinflammation observed in OVX mice. Collectively, these results suggest that peripheral immune stimulation drives neuroinflammation in the hippocampus, which likely contributes to sickness-related behaviors that are further amplified by OVX.

Estrogens did not appear to regulate microglial morphological characteristics in the analyzed hippocampal subfields. Microglial reactivity is a complex process, and assessing changes in microglial morphology alone do not necessarily correlate with the release of neuroinflammatory mediators (Kozlowski and Weimer, 2012; Verdonk et al., 2016). Prior work has noted that OVX increases microglial soma area and retraction of processes, but this effect was only noted in aged rats (Benedusi et al., 2012). This suggests that decreased estrogen levels alone may not be sufficient to induce microglial morphological alterations. Indeed, we did not observe differences in microglial soma perimeter or branching complexity due to OVX or administration of $E_2$.

Although menopause is a condition that predominantly impacts middle-aged to aged women, this study investigated the impacts of estrogen loss in adult mice. We opted for this approach to examine how estrogens regulate the neuroimmune system without the confound of aging. One reason why we may have noted limited changes in some

neuroimmune parameters following OVX, such as the microglia morphological data, may be because our study was conducted in adult mice. Indeed, age-associated declines in estrogens and progesterone are also linked with alterations in metabolism, vascular function, and cellular senescence (Moreau and Hildreth, 2014; Secomandi et al., 2022; Taddei et al., 1996). Therefore, additional studies should investigate whether estrogen loss in aged rodents induces more robust alterations in overall neuroimmune function and microglial reactivity.

In summary, the present study provides evidence that loss of estrogen due to OVX can prime the neuroimmune system to an immune challenge. OVX mice had greater anxiety-like behaviors at baseline. Additionally, OVX mice had amplified sickness behaviors after an LPS challenge that were ameliorated by $E_2$ replacement. The behavioral impairments in OVX mice were accompanied by downregulation of the microglial marker *Cx3cr1*, suggesting that estrogen loss may disinhibit and sensitize microglia to a subsequent immune stimulus. In addition, the expression of pro-inflammatory mRNAs from micropunched CA1 hippocampal subfield were exacerbated in LPS-treated OVX mice and ameliorated with $E_2$ administration. Future studies should further elucidate the mechanisms by which estrogens modulate microglial reactivity and neuroinflammation, which could aid in developing therapies for ameliorating neuroinflammatory diseases and disorders.

## Author contributions

L.K.F. and K.S. conceived and planned the experiments. K.S., S.L.W., R.K., J.S.D., and L.K.F carried out the *in vivo* portion of the study. K.S. performed immunohistochemistry. K.S., S.L.W., R.K., and C.S.H. acquired microscopy images. K.S., S.L.W., and R.K. performed microglial morphological analyses. K.S., S.L.W., R.K., and L.K.F. analyzed the data. K.S. prepared the figures and wrote the manuscript text with support from L.K.F. All authors discussed the results and reviewed the manuscript.

## Declaration of competing interest

The authors declare that they have no known competing financial interests or personal relationships that could have appeared to influence the work reported in this paper.

The authors do not have any competing interests to declare.

## Data availability

Data will be made available on request.

## Acknowledgements

The authors would like to thank The University of Texas at Austin, College of Pharmacy for supporting this work through Start-Up Funds to L.K.F. This work was also funded by the National Institutes of Health (R01AG062716 and R01AG078758 to L.K.F. and F31AG072867 to K.S.).

## References

Acosta-Martinez, 2020. Shaping microglial phenotypes through estrogen receptors: relevance to sex-specific neuroinflammatory responses to brain injury and disease. J. Pharmacol. Exp. Ther. 375 (1), 223–236.

Askew, K., Li, K., Olmos-Alonso, A., Garcia-Moreno, F., Liang, Y., Richardson, P., Tipton, T., Chapman, M.A., Riecken, K., Beccari, S., Sierra, A., Molnar, Z., Cragg, M. S., Garaschuk, O., Perry, V.H., Gomez-Nicola, D., 2017. Coupled proliferation and apoptosis maintain the rapid turnover of microglia in the adult brain. Cell Rep. 18, 391–405.

Au, A., Feher, A., McPhee, L., Jessa, A., Oh, S., Einstein, G., 2016. Estrogens, inflammation and cognition. Front. Neuroendocrinol. 40, 87–100.

Bailey, K.R., Crawley, J.N., 2009. Anxiety-related behaviors in mice. In: Buccafusco, J.J. (Ed.), Methods of Behavior Analysis in Neuroscience, Boca Raton (FL).

Bellesi, M., de Vivo, L., Chini, M., Gilli, F., Tononi, G., Cirelli, C., 2017. Sleep loss promotes astrocytic phagocytosis and microglial activation in mouse cerebral cortex. J. Neurosci. 37, 5263–5273.

Benedusi, V., Meda, C., Della Torre, S., Monteleone, G., Vegeto, E., Maggi, A., 2012. A lack of ovarian function increases neuroinflammation in aged mice. Endocrinology 153, 2777–2788.

Benusa, S.D., George, N.M., Dupree, J.L., 2020. Microglial heterogeneity: distinct cell types or differential functional adaptation? Neuroimmunol. Neuroinflammation 7, 248–263.

Brown, S.L., Fredrickson, B.L., Wirth, M.M., Poulin, M.J., Meier, E.A., Heaphy, E.D., Cohen, M.D., Schultheiss, O.C., 2009. Social closeness increases salivary progesterone in humans. Horm. Behav. 56, 108–111.

Butler, K.G., 2018. Relationship between the cortisol-estradiol phase difference and affect in women. J. Circadian Rhythms 16, 3.

Campagno, K.E., Lu, W., Jassim, A.H., Albalawi, F., Cenaj, A., Tso, H.Y., Clark, S.P., Sripinun, P., Gomez, N.M., Mitchell, C.H., 2021. Rapid morphologic changes to microglial cells and upregulation of mixed microglial activation state markers induced by P2X7 receptor stimulation and increased intraocular pressure. J. Neuroinflammation 18, 217.

Colpo, G.D., Leboyer, M., Dantzer, R., Trivedi, M.H., Teixeira, A.L., 2018. Immune-based strategies for mood disorders: facts and challenges. Expert Rev. Neurother. 18, 139–152.

Dang, R., Guo, Y.Y., Zhang, K., Jiang, P., Zhao, M.G., 2019. Predictable chronic mild stress promotes recovery from LPS-induced depression. Mol. Brain 12, 42.

Dantzer, R., O'Connor, J.C., Freund, G.G., Johnson, R.W., Kelley, K.W., 2008. From inflammation to sickness and depression: when the immune system subjugates the brain. Nat. Rev. Neurosci. 9, 46–56.

Davis, B.M., Salinas-Navarro, M., Cordeiro, M.F., Moons, L., De Groef, L., 2017. Characterizing microglia activation: a spatial statistics approach to maximize information extraction. Sci. Rep. 7, 1576.

Espinosa-Garcia, C., Sayeed, I., Yousuf, S., Atif, F., Sergeeva, E.G., Neigh, G.N., Stein, D. G., 2017. Stress primes microglial polarization after global ischemia: therapeutic potential of progesterone. Brain Behav. Immun. 66, 177–192.

Fernandez-Arjona, M.D.M., Grondona, J.M., Granados-Duran, P., Fernandez-Llebrez, P., Lopez-Avalos, M.D., 2017. Microglia morphological categorization in a rat model of neuroinflammation by hierarchical cluster and principal components analysis. Front. Cell. Neurosci. 11, 235.

Fonken, L.K., Frank, M.G., Kitt, M.M., D'Angelo, H.M., Norden, D.M., Weber, M.D., Barrientos, R.M., Godbout, J.P., Watkins, L.R., Maier, S.F., 2016. The alarmin HMGB1 mediates age-induced neuroinflammatory priming. J. Neurosci. 36 (30), 7946–7956.

Forbes-Lorman, R.M., 2021. Sex-specific effects of neonatal progestin receptor antagonism on juvenile social play behavior in rats. Behav. Brain Funct. 17, 10.

Frye, C.A., Llaneza, D.C., Walf, A.A., 2009. Progesterone can enhance consolidation and/or performance in spatial, object and working memory tasks in Long-Evans rats. Anim. Behav. 78, 279–286.

Gabbita, S.P., Srivastava, M.K., Eslami, P., Johnson, M.F., Kobritz, N.K., Tweedie, D., Greig, N.H., Zemlan, F.P., Sharma, S.P., Harris-White, M.E., 2012. Early intervention with a small molecule inhibitor for tumor necrosis factor-alpha prevents cognitive deficits in a triple transgenic mouse model of Alzheimer's disease. J. Neuroinflammation 9, 99.

Ghisletti, S., Meda, C., Maggi, A., Vegeto, E., 2005. 17beta-estradiol inhibits inflammatory gene expression by controlling NF-kappaB intracellular localization. Mol. Cell Biol. 25, 2957–2968.

Gresack, J.E., Frick, K.M., 2006. Effects of continuous and intermittent estrogen treatments on memory in aging female mice. Brain Research 1115, 135–147.

Hara, Y., Waters, E.M., McEwen, B.S., Morrison, J.H., 2015. Estrogen effects on cognitive and synaptic health over the lifecourse. Physiol. Rev. 95, 785–807.

Hart, B.L., 1988. Biological basis of the behavior of sick animals. Neurosci. Biobehav. Rev. 12, 123–137.

Hennessy, M.B., Deak, T., Schiml, P.A., 2014. Sociality and sickness: have cytokines evolved to serve social functions beyond times of pathogen exposure? Brain Behav. Immun. 37, 15–20.

Henry, C.J., Huang, Y., Wynne, A., Hanke, M., Himler, J., Bailey, M.T., Sheridan, J.F., Godbout, J.P., 2008. Minocycline attenuates lipopolysaccharide (LPS)-induced neuroinflammation, sickness behavior, and anhedonia. J. Neuroinflammation 5.

Henry, C.J., Huang, Y., Wynne, A.M., Godbout, J.P., 2009. Peripheral lipopolysaccharide (LPS) challenge promotes microglial hyperactivity in aged mice that is associated with exaggerated induction of both pro-inflammatory IL-1beta and anti-inflammatory IL-10 cytokines. Brain Behav. Immun. 23, 309–317.

Ivy, A.S., Rex, C.S., Chen, Y., Dube, C., Maras, P.M., Grigoriadis, D.E., Gall, C.M., Lynch, G., Baram, T.Z., 2010. Hippocampal dysfunction and cognitive impairments provoked by chronic early-life stress involve excessive activation of CRH receptors. J. Neurosci. 30, 13005–13015.

Kessler, R.C., 2003. Epidemiology of women and depression. J. Affect. Disord. 74, 5–13.

Kim, Y.K., Na, K.S., Myint, A.M., Leonard, B.E., 2016. The role of pro-inflammatory cytokines in neuroinflammation, neurogenesis and the neuroendocrine system in major depression. Prog. Neuro-Psychopharmacol. Biol. Psychiatry 64, 277–284.

Klein, S.L., Flanagan, K.L., 2016. Sex differences in immune responses. Nat. Rev. Immunol. 16, 626–638.

Kokiko-Cochran, O.N., Godbout, J.P., 2018. The inflammatory continuum of traumatic brain injury and alzheimer's disease. Front. Immunol. 9, 672.

Kopitar-Jerala, N., 2015. Innate immune response in brain, NF-kappa B signaling and cystatins. Front. Mol. Neurosci. 8, 73.

Kozlowski, C., Weimer, R.M., 2012. An automated method to quantify microglia morphology and application to monitor activation state longitudinally in vivo. PLoS One 7, e31814.

Kurachi, H., Adachi, H., Ohtsuka, S., Morishige, K., Amemiya, K., Keno, Y., Shimomura, I., Tokunaga, K., Miyake, A., Matsuzawa, Y., et al., 1993. Involvement

of epidermal growth factor in inducing obesity in ovariectomized mice. Am. J. Physiol. 265, E323–E331.
Lawson, L.J., Perry, V.H., Dri, P., Gordon, S., 1990. Heterogeneity in the distribution and morphology of microglia in the normal adult mouse brain. Neuroscience 39, 151–170.
Lenz, K.M., McCarthy, M.M., 2015. A starring role for microglia in brain sex differences. Neuroscientist 21, 306–321.
Liu, Y., Zhang, Y., Zheng, X., Fang, T., Yang, X., Luo, X., Guo, A., Newell, K.A., Huang, X. F., Yu, Y., 2018. Galantamine improves cognition, hippocampal inflammation, and synaptic plasticity impairments induced by lipopolysaccharide in mice. J. Neuroinflammation 15, 112.
Maner, J.K., Miller, S.L., 2014. Hormones and social monitoring: menstrual cycle shifts in progesterone underlie women's sensitivity to social information. Evol. Hum. Behav. 35, 9–16.
McNatty, K.P., Makris, A., DeGrazia, C., Osathanondh, R., Ryan, K.J., 1979. The production of progesterone, androgens, and estrogens by granulosa cells, thecal tissue, and stromal tissue from human ovaries in vitro. J. Clin. Endocrinol. Metab. 49, 687–699.
Mizobuchi, H., Soma, G.I., 2021. Low-dose lipopolysaccharide as an immune regulator for homeostasis maintenance in the central nervous system through transformation to neuroprotective microglia. Neural Regen Res 16, 1928–1934.
Moreau, K.L., Hildreth, K.L., 2014. Vascular aging across the menopause transition in healthy women. Adv Vasc Med 2014.
Muccigrosso, M.M., Ford, J., Benner, B., Moussa, D., Burnsides, C., Fenn, A.M., Popovich, P.G., Lifshitz, J., Walker, F.R., Eiferman, D.S., Godbout, J.P., 2016. Cognitive deficits develop 1month after diffuse brain injury and are exaggerated by microglia-associated reactivity to peripheral immune challenge. Brain Behav. Immun. 54, 95–109.
Murphy, A.J., Guyre, P.M., Pioli, P.A., 2010. Estradiol suppresses NF-kappa B activation through coordinated regulation of let-7a and miR-125b in primary human macrophages. J. Immunol. 184, 5029–5037.
Niraula, A., Sheridan, J.F., Godbout, J.P., 2017. Microglia priming with aging and stress. Neuropsychopharmacology 42, 318–333.
O'Neil, S.M., Witcher, K.G., McKim, D.B., Godbout, J.P., 2018. Forced turnover of aged microglia induces an intermediate phenotype but does not rebalance CNS environmental cues driving priming to immune challenge. Acta Neuropathol Commun 6, 129.
Pawelec, P., Ziemka-Nalecz, M., Sypecka, J., Zalewska, T., 2020. The impact of the cx3cl1/cx3cr1 Axis in neurological disorders. Cells 9.
Posillico, C.K., Garcia-Hernandez, R.E., Tronson, N.C., 2021. Sex differences and similarities in the neuroimmune response to central administration of poly I:C. J. Neuroinflammation 18, 193.
Price, J.L., Drevets, W.C., 2010. Neurocircuitry of mood disorders. Neuropsychopharmacology 35, 192–216.
Rhie, S.J., Jung, E.Y., Shim, I., 2020. The role of neuroinflammation on pathogenesis of affective disorders. J Exerc Rehabil 16, 2–9.
Rogers, N.H., Perfield 2nd, J.W., Strissel, K.J., Obin, M.S., Greenberg, A.S., 2009. Reduced energy expenditure and increased inflammation are early events in the development of ovariectomy-induced obesity. Endocrinology 150, 2161–2168.
Rubinow, D.R., Schmidt, P.J., 2019. Sex differences and the neurobiology of affective disorders. Neuropsychopharmacology 44, 111–128.
Sagsoz, N., Oguzturk, O., Bayram, M., Kamaci, M., 2001. Anxiety and depression before and after the menopause. Arch. Gynecol. Obstet. 264, 199–202.
Sanchez, K., Darling, J.S., Kakkar, R., Wu, S.L., Zentay, A., Lowry, C.A., Fonken, L.K., 2022. Mycobacterium vaccae immunization in rats ameliorates features of age-associated microglia activation in the amygdala and hippocampus. Sci. Rep. 12, 2165.
Santollo, J., Torregrossa, A.M., Eckel, L.A., 2011. Estradiol acts in the medial preoptic area, arcuate nucleus, and dorsal raphe nucleus to reduce food intake in ovariectomized rats. Horm. Behav. 60, 86–93.
Savage, J.C., St-Pierre, M.K., Hui, C.W., Tremblay, M.E., 2019. Microglial ultrastructure in the Hippocampus of a lipopolysaccharide-induced sickness mouse model. Front. Neurosci. 13, 1340.
Scheggi, S., De Montis, M.G., Gambarana, C., 2018. Making sense of rodent models of anhedonia. Int. J. Neuropsychopharmacol. 21, 1049–1065.
Schwarz, J.M., Bilbo, S.D., 2012. Sex, glia, and development: interactions in health and disease. Horm. Behav. 62, 243–253.
Secomandi, L., Borghesan, M., Velarde, M., Demaria, M., 2022. The role of cellular senescence in female reproductive aging and the potential for senotherapeutic interventions. Hum. Reprod. Update 28, 172–189.
Seibenhener, M.L., Wooten, M.C., 2015. Use of the Open Field Maze to measure locomotor and anxiety-like behavior in mice. J. Vis. Exp., e52434
Szentirmai, E., Krueger, J.M., 2014. Sickness behaviour after lipopolysaccharide treatment in ghrelin deficient mice. Brain Behav. Immun. 36, 200–206.
Taddei, S., Virdis, A., Ghiadoni, L., Mattei, P., Sudano, I., Bernini, G., Pinto, S., Salvetti, A., 1996. Menopause is associated with endothelial dysfunction in women. Hypertension 28, 576–582.
Tapp, Z.M., Godbout, J.P., Kokiko-Cochran, O.N., 2019. A tilted Axis: maladaptive inflammation and HPA Axis dysfunction contribute to consequences of TBI. Front. Neurol. 10, 345.
Tarr, A.J., Chen, Q., Wang, Y., Sheridan, J.F., Quan, N., 2012. Neural and behavioral responses to low-grade inflammation. Behav. Brain Res. 235, 334–341.
Vegeto, E., Belcredito, S., Etteri, S., Ghisletti, S., Brusadelli, A., Meda, C., Krust, A., Dupont, S., Ciana, P., Chambon, P., Maggi, A., 2003. Estrogen receptor-alpha mediates the brain antiinflammatory activity of estradiol. Proc. Natl. Acad. Sci. U. S. A. 100, 9614–9619.
Vegeto, E., Benedusi, V., Maggi, A., 2008. Estrogen anti-inflammatory activity in brain: a therapeutic opportunity for menopause and neurodegenerative diseases. Front. Neuroendocrinol. 29, 507–519.
Velez-Perez, A., Holder, M.K., Fountain, S., Blaustein, J.D., 2020. Estradiol increases microglial response to lipopolysaccharide in the ventromedial hypothalamus during the peripubertal sensitive period in female mice. eNeuro 7.
Verdonk, F., Roux, P., Flamant, P., Fiette, L., Bozza, F.A., Simard, S., Lemaire, M., Plaud, B., Shorte, S.L., Sharshar, T., Chretien, F., Danckaert, A., 2016. Phenotypic clustering: a novel method for microglial morphology analysis. J. Neuroinflammation 13, 153.
Vieira Potter, V.J., Strissel, K.J., Xie, C., Chang, E., Bennett, G., Defuria, J., Obin, M.S., Greenberg, A.S., 2012. Adipose tissue inflammation and reduced insulin sensitivity in ovariectomized mice occurs in the absence of increased adiposity. Endocrinology 153, 4266–4277.
Villa, A., Vegeto, E., Poletti, A., Maggi, A., 2016. Estrogens, neuroinflammation, and neurodegeneration. Endocr. Rev. 37, 372–402.
Wolf, Y., Yona, S., Kim, K.W., Jung, S., 2013. Microglia, seen from the CX3CR1 angle. Front. Cell. Neurosci. 7, 26.
Yang, Y., Kozloski, M., 2011. Sex differences in age trajectories of physiological dysregulation: inflammation, metabolic syndrome, and allostatic load. J Gerontol A Biol Sci Med Sci 66, 493–500.
Yeh, C.H., Hsieh, L.P., Lin, M.C., Wei, T.S., Lin, H.C., Chang, C.C., Hsing, C.H., 2018. Dexmedetomidine reduces lipopolysaccharide induced neuroinflammation, sickness behavior, and anhedonia. PLoS One 13, e0191070.
Yew, W.P., Djukic, N.D., Jayaseelan, J.S.P., Walker, F.R., Roos, K.A.A., Chataway, T.K., Muyderman, H., Sims, N.R., 2019. Early treatment with minocycline following stroke in rats improves functional recovery and differentially modifies responses of peri-infarct microglia and astrocytes. J. Neuroinflammation 16, 6.
Young, K., Morrison, H., 2018. Quantifying microglia morphology from photomicrographs of immunohistochemistry prepared tissue using ImageJ. J. Vis. Exp. 136, 57648.
Zhao, J.Y., Bi, W., Xiao, S., Lan, X., Cheng, X.F., Zhang, J.W., Lu, D.X., Wei, W., Wang, Y. P., Li, H.M., Fu, Y.M., Zhu, L.H., 2019. Neuroinflammation induced by lipopolysaccharide causes cognitive impairment in mice. Sci Rep-Uk 9.